

THERMAL HISTORY OF UREILITE, PECORA ESCARPMENT 82506 DEDUCED FROM CATION DISTRIBUTION AND DIFFUSION PROFILE OF MINERALS

Hiromi TOYODA¹, Nobuhiko HAGA¹, Osamu TACHIKAWA¹,
Hiroshi TAKEDA¹ and Teruaki ISHII²

¹*Mineralogical Institute, Faculty of Science, University of Tokyo,
3-1, Hongo 7-chome, Bunkyo-ku, Tokyo 113*

²*Ocean Research Institute, University of Tokyo,
15-1, Minamidai 1-chome, Nakano-ku, Tokyo 164*

Abstract: PCA82506 is relatively unshocked compared with most ureilites. Large unshocked pigeonite and olivine crystals were studied by means of single crystal X-ray diffraction, analytical TEM, optical microscope and an electronprobe. The chemical compositions of the PCA82506 pigeonites are $\text{Ca}_6\text{Mg}_{76}\text{Fe}_{18}$, while the average olivine core composition is Fa_{20} . A region about 50 micrometer apart from the olivine rim is reduced by the carbonaceous (C) matrix. From the diffusion profiles of olivine crystals, a cooling rate of 10–15°C/h is estimated by the computer simulation method of MIYAMOTO *et al.* (Proc. Lunar Planet. Sci. Conf., 16th, Pt. 1, D116, 1985). The cell dimensions of the PCA82506 pigeonite determined from 23 reflections are: a, 9.6649(9); b, 8.8719(6); c, 5.2134(5)Å; and β , 108.51(6)°. The site occupancy factors are M1 (Mg 0.064, Fe 0.936) and M2 (Ca 0.116, Mg 0.568, Fe 0.316). This cation distribution gives an equilibrium temperature of 800°C by plotting the K value of PCA82506 on the distribution isotherm of SAXENA *et al.* (Earth Planet. Sci. Lett., **21**, 194, 1974). The PCA82506 pigeonites may have cooled more rapidly than terrestrial pigeonites from the Isle of Mull and almost as rapid as the most rapidly cooled mare basalts.

1. Introduction

Pecora Escarpment 82506 (PCA82506) is a new Antarctic ureilite, consisting of coarse-grained pigeonite, olivine and carbonaceous matrix. Ureilite pigeonites are more Mg-rich than the terrestrial ones and show no evidence of exsolution and inversion in spite of their well developed plutonic texture. The high Ca content in olivine suggests a high temperature origin (BERKLEY *et al.*, 1980). Shock textures such as translation gliding and kink bands are common. From these features, it is generally understood that most ureilites experienced a high temperature condition, a shock event, and then rapid cooling (BERKLEY *et al.*, 1980). Evidence of the shock events is the presence of lonsdaleite and diamond.

Four major hypotheses of the ureilite origin have been proposed: (a) shock recrystallization of carbonaceous chondrites (VDOVYKEN, 1970); (b) partial melt residues, into which C matrix was introduced later, possibly in a shock event (BOYNTON *et al.*, 1976); (c) cumulate ultramafic rocks, with an abundant primary component (BERKLEY *et al.*, 1980); (d) crystallization from partially melted, gravitationally frac-

tionated products in the nebula (TAKEDA and TACHIKAWA, 1984).

The current problems of the ureilite genesis are the time when the silicates and carbonaceous matrix were mixed and the manner in which the primordial noble gases were trapped. Recently, BERKLEY *et al.* (1980) proposed the detailed model which is based on the assumption that ureilites are cumulated rocks. However, BEGEMANN and OTT (1983) pointed out that his model cannot explain the problem of the noble gases.

In spite of the large crystal size and uniform chemical composition of the ureilite pigeonite, no good single crystal has been available for single crystal X-ray diffraction study. Fortunately, single crystals in PCA82506 are suitable for detailed mineralogical and crystallographic study. This work has been undertaken to investigate mineralogy, chemistry and crystallograph of the PCA82506 ureilite to obtain its thermal history. Related samples, Yamato-790981 and ALH-81101, have been examined also in the hope that it might reveal their origin, evolution and thermal histories.

2. Samples and Experimental Techniques

PCA82506 is relatively unshocked compared with most ureilites (MASON, *Antarct. Meteorite Newsl.*, 1983). Large unshocked crystals were selected from the chip of PCA82506,13 and examined by means of single crystal X-ray diffraction, electron microprobe, and analytical transmission electron microscope (ATEM). Polished thin sections (PTS) of PCA82506,24, ALH-81101,12 and Y-790981,42 were also studied with an optical microscope and an electronprobe (JEOL 733).

Two olivine crystals which had carbon coated surfaces nearly perpendicular to the plane of the PTS were analyzed at intervals of 4 micrometer from core to rim

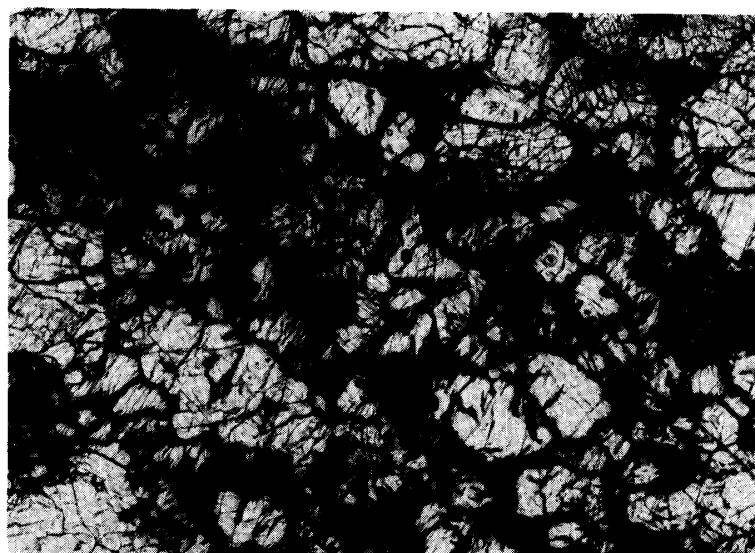
Table 1. Crystal data and experimental conditions for single crystal data collection for pigeonite.

| | |
|---|---|
| Space group | P2 ₁ /c |
| Cell dimensions (Å) | a, 9.6649(9); b, 8.8719(6); c, 5.2134(5); $\beta = 108.509(6)^\circ$ |
| Absorption coefficients (cm ⁻¹) | 31 |
| Wave length λ (Å) | Mo K α = 0.71069 |
| Monochromator | graphite |
| Temperature (K) | 298 |
| Diffractometer | RIGAKU AFC5 160 mA/50 kV |
| Scan mode | 2 θ - ω scan |
| Scan width (°) | 1.0+0.5 tan θ |
| Scan speed (°/min) in ω | 5 |
| Collimator ϕ (mm) | 0.75 |
| sin θ/λ (A-1) | 1.0 |
| Reciprocal space covered | 1/4 |
| Number of observations | 3341 |
| Peak reflections | F \geq 2.5 σ (F) |
| Extinction | no |
| Scattering factors | International Table Vol. 4 |
| Anomalous scattering | not included |
| Weighting scheme | 1/ σ^2 (F) |

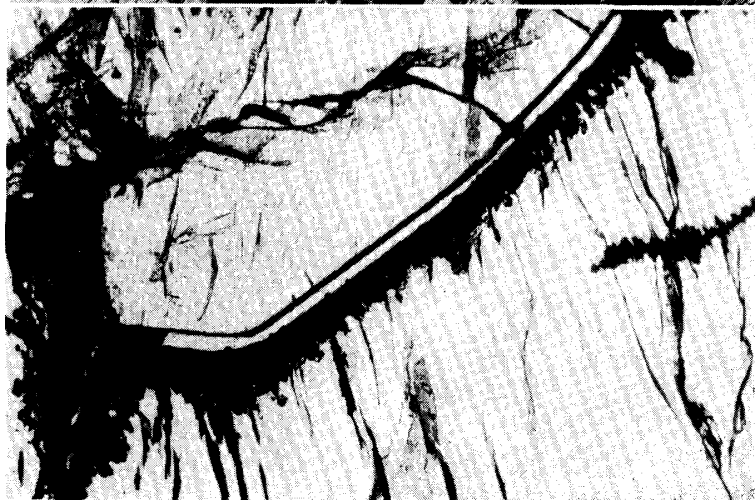
parallel to cleavages that could be assumed to be parallel to [001]. A modal abundance of phases was obtained from the analyses over the entire thin section on a $0.2\text{ mm} \times 0.5\text{ mm}$ grid spacing.

Chemical compositions of submicroscopic phases were determined using a Hitachi H-600 ATEM with a Kevex EDS system operated at 100 kV and 0.1 mA beam current. These data were reduced using the k-factor technique of CLIFF and LORIMER (1975) with the total weight percentage of oxides normalized to 100%.

Diffraction intensities for a 0.2 mm equidimensional pigeonite crystal were obtained with a 4-circle single crystal diffractometer under the conditions outlined in Table 1. To obtain site occupancy factors for Mg and Fe in the M1 and M2 sites of pigeonite, the structure refinement was carried out with the full-matrix least squares program RADY (program modified by SASAKI, 1982) using 2255 reflections ($F \geq 2.5\sigma(F)$). Starting parameters were those from the previous structural work of TAKEDA (1972).



a. Polished thin section of PCA82506,24. Width 12 mm.



b. Olivine rim where diffusion profiles were obtained. Carbon matrix crept along cleavages. Width 0.95 mm.

Fig. 1. Photomicrographs of PCA82506. Plain light.

3. Results

3.1. Mineralogy of PCA82506

PCA82506 is relatively unshocked (Fig. 1a), and shows a modal abundance as obtained by line analyses, olivine (50%), pigeonite (45%) and dark C-bearing matrix (5%). Several grains of olivine show undulatory extinction and some pigeonite crystals display (100) twinning. Quantitative microprobe analysis indicated that pigeonite grains are very homogeneous at $\text{Ca}_8\text{Mg}_{76}\text{Fe}_{18}$ (Fig. 2, Table 2). MnO/FeO ratios (wt%) of pigeonite are plotted within the almost horizontal trend of Y-790981

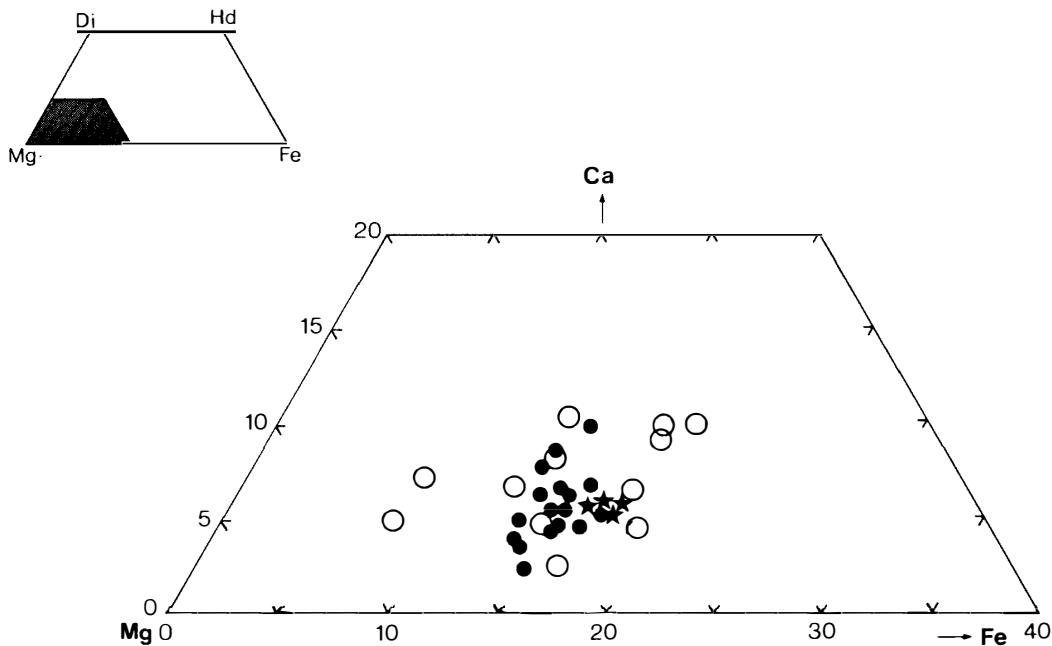


Fig. 2. Chemical compositions of pyroxenes plotted in a part of a pyroxene quadrilateral. Open circle: known ureilites (BERKLEY *et al.*, 1978; TAKEDA *et al.*, 1980), star: PCA82506, filled circle: ALH-81101. Shaded area is enlarged.

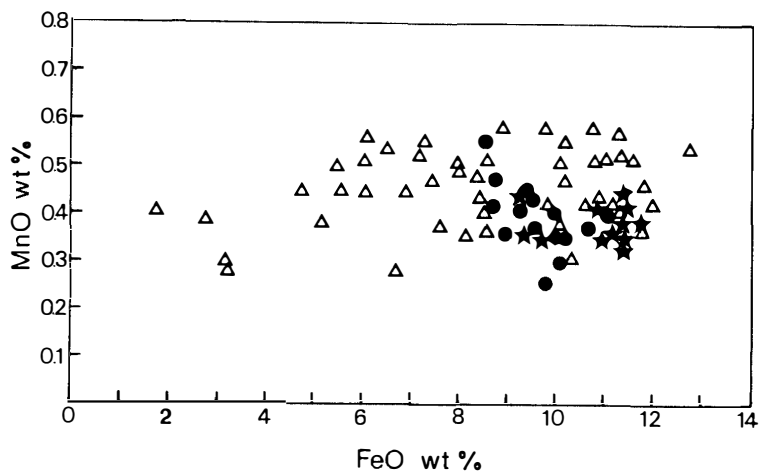


Fig. 3. A plot of MnO/FeO ratio (wt%) for PCA82506, ALH-81101 and Y-790981. Star: PCA82506, filled circle: ALH-81101, open triangle: Y-790981.

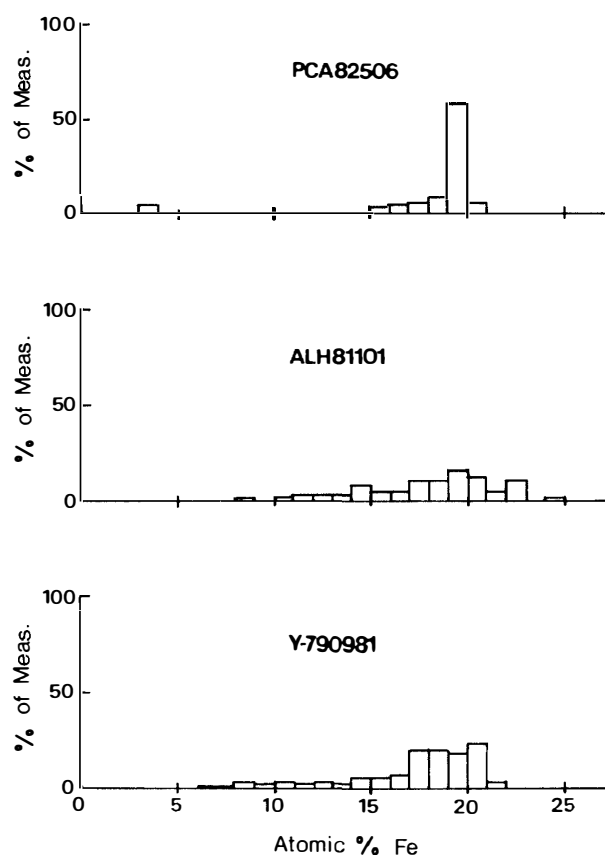


Fig. 4. Chemical compositions of olivines of PCA82506, ALH-81101 and Y-790981.

Table 2. Chemical compositions (wt%) of pyroxenes and olivines.

| Sample | PCA82506 | | ALH-81101 | | | | Y-790981 | |
|--------------------------------|----------|-------|-----------|--------|--------|-------|----------|-------|
| | Pig. | Ol. | Pig. 1 | Pig. 2 | Pig. 3 | Ol. | Pig. | Ol. |
| SiO ₂ | 55.01 | 38.48 | 55.75 | 55.51 | 55.54 | 38.75 | 54.53 | 40.02 |
| TiO ₂ | 0.03 | | 0.03 | | | | 0.09 | 0.01 |
| Al ₂ O ₃ | 0.69 | 0.14 | 0.28 | 0.09 | 0.24 | 0.06 | 1.27 | 0.06 |
| FeO | 11.48 | 18.78 | 8.77 | 10.03 | 9.36 | 17.96 | 11.43 | 11.57 |
| MnO | 0.38 | 0.37 | 0.46 | 0.42 | 0.40 | 0.43 | 0.45 | 0.56 |
| MgO | 27.58 | 40.46 | 29.18 | 29.99 | 30.98 | 41.56 | 26.36 | 46.73 |
| CaO | 2.97 | 0.35 | 4.29 | 2.31 | 1.98 | 0.39 | 4.38 | 0.31 |
| Na ₂ O | 0.08 | 0.04 | 0.05 | 0.02 | 0.04 | 0.03 | 0.14 | 0.03 |
| K ₂ O | | | 0.02 | | 0.03 | 0.01 | | 0.01 |
| Cr ₂ O ₃ | 1.20 | 0.74 | 1.09 | 1.00 | 1.15 | 0.69 | 1.18 | 0.65 |
| Total | 99.42 | 99.36 | 99.92 | 99.37 | 99.72 | 99.88 | 99.83 | 99.95 |

and close to the ALH-81101 region (Fig. 3). The olivines are uniform within the grain except at the rim, and an average olivine core composition is Fa₂₀ (Fig. 4), but the area about 50 micrometer from the rim is reduced by C-bearing matrix. Mg increases toward the rim.

3.2. Diffusion profiles of olivine crystal

The reverse zoning at grain boundaries of ureilite olivines is generally thought

to be due to reduction by the C-bearing matrix. To estimate the cooling rate, the compositional profiles, 50–20 microns away from the rim of PCA82506 olivine (Fig. 1b), were compared with calculated profiles by computer simulation (MIYAMOTO *et al.*, 1985). The following assumptions were made: (1) iron diffusion in olivine controls the formation of the zoning profile; (2) both temperature and concentration dependence of the diffusion coefficient (BUENING and BUSECK, 1973) were considered in the diffusion equation; (3) the boundary condition is that the Fa content at the edge of the grain is zero; (4) the initial profile is a step function; (5) the olivine grain was approximated as sphere. To fit the calculated profile to the observed profile, the linear cooling rates from the initial temperature (1300, 1250, 1200, 1150°C) to 800°C were calculated. The initial temperature (1150 to 1250°C) was estimated from the chemical compositions of three coexisting pyroxenes in Yamato-74130 (TAKEDA and YANAI, 1982) and the pyroxene geothermometer of LINDSLEY and ANDERSON (1983). The details of the method and results are given in a separate paper (MIYAMOTO *et al.*, 1985). As a result, it is inferred that PCA82506 experienced a rapid cooling at a rate of 10–15°C/h.

3.3. Precession photographs

Several crystals up to 0.8 mm in diameter were separated from a small chip, PCA82506,13 and examined with an X-ray precession camera to identify the orientation and to estimate the degree of shock deformation. The $h0l$ and $0kl$ nets of pyroxene were taken using Zr-filtered Mo-K α radiation (40 kV, 15 mA).

The diffraction pattern of pigeonite shows minor twinning on (100) in some crystals and weak diffuse streaks parallel to [100]*. Overall, the diffractions are relatively sharp in comparison with those of pigeonites from other ureilites.

3.4. Crystal structure analysis of the PCA82506 pigeonite

After three cycles of isotropic refinement using average values of atomic scattering factors of Mg and Fe for the M1 and M2 sites, an R value became 0.119. Four additional cycles of refinement by varying the anisotropic thermal parameters and site occupancy parameters of the M sites gave a final R value of 0.080. Final positional and thermal parameters are listed in Tables 3 and 4. The site occupancy factors of PCA82506 are M1 (Mg 0.064, Fe 0.936) and M2 (Ca 0.116, Mg 0.568, Fe 0.316), and are compared with other published data in Table 5.

Table 3. Atomic coordinates, equivalent isotropic temperature factors of PCA82506 pigeonite.

| Atom | x | y | z | B_{eq} |
|------|------------|-------------|------------|----------|
| M1 | 0.2507 (1) | 0.6542 (1) | 0.2249 (2) | 0.77 (3) |
| M2 | 0.2560 (1) | 0.01781 (9) | 0.2231 (2) | 1.09 (2) |
| SiA | 0.0427 (1) | 0.34084 (9) | 0.2846 (2) | 0.70 (2) |
| SiB | 0.5508 (1) | 0.8375 (1) | 0.2346 (2) | 0.69 (2) |
| O1A | 0.8670 (3) | 0.3388 (2) | 0.1761 (4) | 0.84 (5) |
| O1B | 0.3746 (3) | 0.8382 (2) | 0.1290 (4) | 0.84 (5) |
| O2A | 0.1217 (3) | 0.5008 (2) | 0.3256 (5) | 0.93 (6) |
| O2B | 0.6311 (3) | 0.9859 (3) | 0.3791 (5) | 1.13 (7) |
| O3A | 0.1053 (3) | 0.2714 (3) | 0.5957 (5) | 1.12 (6) |
| O3B | 0.6049 (3) | 0.7023 (3) | 0.4691 (5) | 1.06 (6) |

Table 4. Anisotropic temperature factors ($\times 10^3$) of PCA82506 pigeonite.

| Atom | β_{11} | β_{22} | β_{33} | β_{12} | β_{13} | β_{23} |
|------|--------------|--------------|--------------|--------------|--------------|--------------|
| M1 | 3.3 (1) | 1.60 (9) | 6.8 (3) | -0.04 (9) | 1.4 (1) | 0.1 (1) |
| M2 | 4.09 (8) | 3.45 (9) | 7.5 (2) | 0.58 (7) | 1.3 (1) | 1.2 (1) |
| SiA | 3.00 (8) | 1.47 (7) | 6.8 (2) | -0.19 (7) | 1.7 (1) | -0.2 (1) |
| SiB | 2.93 (8) | 1.57 (7) | 6.1 (2) | -0.12 (7) | 1.6 (1) | -0.3 (1) |
| O1A | 3.2 (2) | 2.4 (2) | 7.0 (6) | 0.3 (2) | 1.5 (3) | 0.4 (3) |
| O1B | 2.8 (2) | 2.6 (2) | 7.9 (6) | -0.1 (2) | 1.5 (3) | 0.0 (3) |
| O2A | 4.3 (2) | 1.9 (2) | 8.1 (6) | -0.7 (2) | 2.3 (3) | 0.2 (3) |
| O2B | 4.5 (3) | 2.6 (2) | 13.1 (8) | -1.3 (2) | 3.9 (4) | -2.5 (3) |
| O3A | 4.0 (2) | 3.2 (2) | 11.3 (7) | 0.4 (2) | 2.8 (4) | 2.8 (3) |
| O3B | 3.7 (2) | 3.4 (2) | 9.0 (7) | 0.3 (2) | 1.9 (3) | 2.6 (3) |

Table 5. Composition, cation distribution coefficient (K) and equilibration temperature of pigeonites.

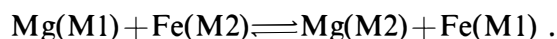
| No. | Sample | Composition | | | K | Method | C.E.T. (a) °C | C.E.T. (b) °C | Reference |
|-----|--------------|-------------|------|------|-------|-----------|---------------------|---------------------|-----------|
| | | Wo | En | Fs | | | | | |
| 1 | Mull | 9 | 39 | 52 | 0.031 | X-ray | 500 | | (1) |
| 2 | Mull | 9 | 39 | 52 | 0.045 | X-ray | 500 | 550 | (2) |
| 3 | 10003,38 | 8 | 54 | 38 | 0.09 | X-ray | 600 | 730 | (3) |
| 4 | 12021,150-P1 | 9 | 59 | 32 | 0.081 | Mössbauer | 570 | 710 | (4) |
| 5 | 12018,35-P1 | 14 | 50 | 35 | 0.084 | Mössbauer | 690 | 790 | (4) |
| 6 | 12018,35-P2 | 13 | 46 | 41 | 0.160 | Mössbauer | 1000 | | (4) |
| 7 | 12052 | 9 | 63 | 28 | 0.11 | X-ray | 690 | 860 | (5) |
| 8 | 12053,79-P1 | 11 | 57 | 32 | 0.091 | Mössbauer | 670 | 790 | (4) |
| 9 | 12053,72 | 10.5 | 60.5 | 29 | 0.086 | Mössbauer | 620 | 770 | (6) |
| 10 | 14310,115 | 9 | 64.5 | 26.5 | 0.094 | Mössbauer | 630 | 760 | (6) |
| 11 | 15076 | 6 | 66 | 28 | 0.09 | Mössbauer | 550 | 680 | (7) |
| 12 | 15476 | 6 | 66 | 28 | 0.08 | Mössbauer | 510 | 650 | (7) |
| 13 | 15597,28 | 6 | 68 | 26 | 0.12 | X-ray | 670 | 800 | (8) |
| * | PCA82506,13 | 6 | 76 | 18 | 0.123 | X-ray | 690 | 800 | this work |

C.E.T.(a)=cation equilibration temperature obtained from Fig. 5.

C.E.T.(b)=cation equilibration temperature obtained from Fig. 6.

(1) MORIMOTO and GÜVEN (1970), (2) BROWN *et al.* (1972), (3) CLARK *et al.* (1971), (4) HAFNER *et al.* (1971), (5) TAKEDA (1972), (6) GHOSE *et al.* (1972), (7) VIRGO (1973), (8) BROWN *et al.* (1973).

For a simple binary solution of Fe and Mg, the cation exchange between adjacent M1 and M2 sites can be written as follows:



The distribution coefficient K calculated by a formula

$$K = \frac{\text{Fe(M1)} \cdot \text{Mg(M2)}}{\text{Mg(M1)} \cdot \text{Fe(M2)}} ,$$

is 0.123 for PCA82506 (Table 5). To estimate an apparent equilibrium temperature, the datum of the PCA82506 pigeonite is plotted (Fig. 5) on the distribution isotherm of pigeonite (YAJIMA and HAFNER, 1974) together with the data of Table 5. Then, the data shown in Table 5 are plotted on distribution isotherms of HAFNER *et al.* (1971) (Fig. 6) and of SAXENA *et al.* (1974) (Fig. 7) to estimate the equilibrium temperatures of the PCA82506 pigeonite. The value of 800°C was obtained as the last equilibrium

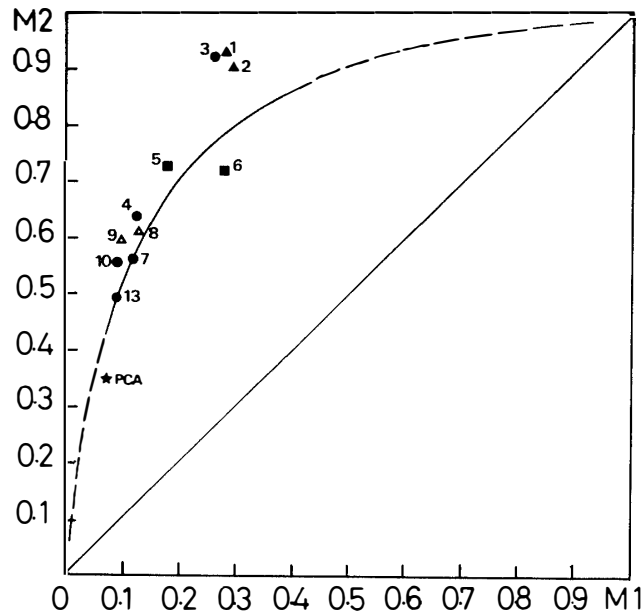


Fig. 5. Distribution isotherm of pigeonites with data of Table 5 except samples 11 and 12 plotted. Numbers same as Table 5. For samples 11 and 12, only K values are given.

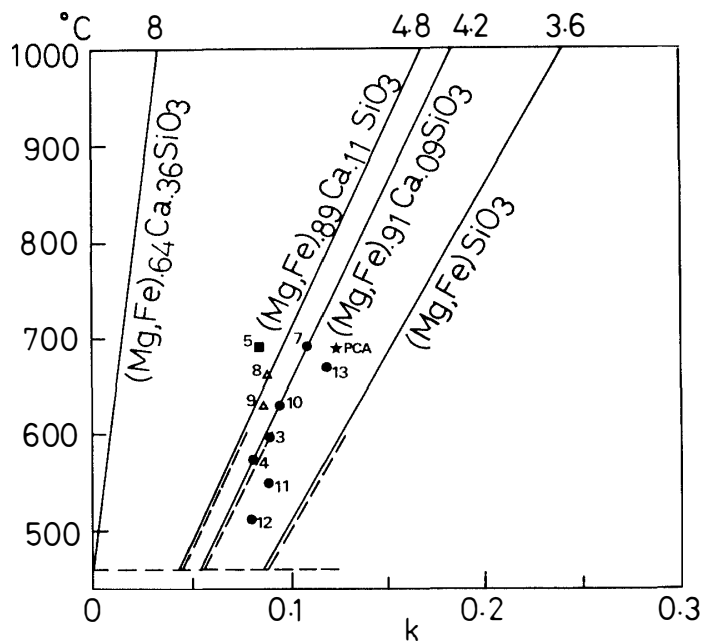


Fig. 6. Distribution isotherm of HAFNER *et al.* (1971) with the data of Table 5 plotted. Numbers same as Table 5. Some data in Table 5 are out of the range of this figure.

temperature of PCA82506 by the distribution isotherm of SAXENA *et al.* (1974).

3.5. TEM and ATEM observation

After the X-ray study, two crystals of pigeonite and one crystal of olivine from PCA82506 were mounted in thick resin with the *b*-axis perpendicular to the plane of a glass slide, and were polished to a thin section. Each crystal was removed from the glass slide and glued to a molybdenum support grid for ion-thinning until perfora-

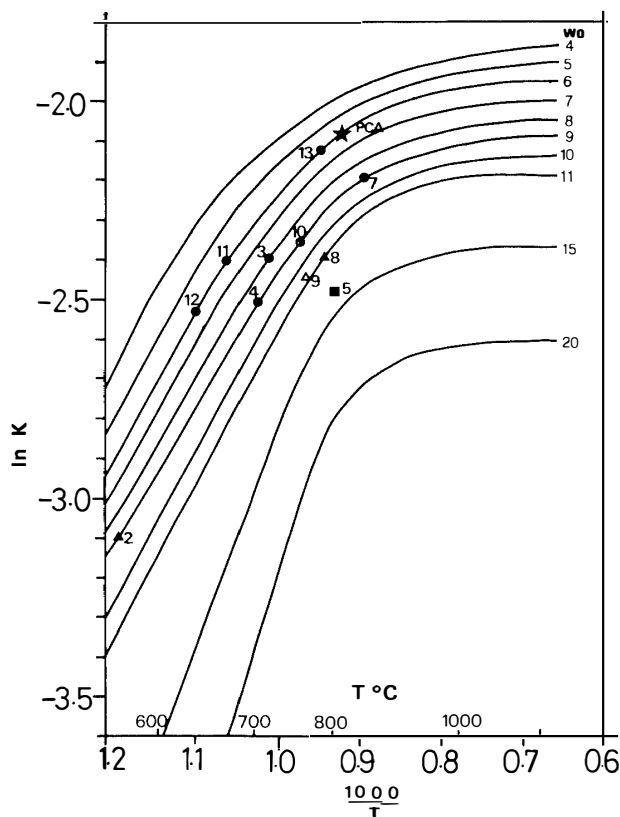


Fig. 7. Distribution isotherm of SAXENA *et al.* (1974) with data of Table 5 plotted. Numbers same as Table 5. Some data in Table 5 are out of this figure.

tion occurred. Electron microscopy of the ion-thinned samples was carried out with a high-resolution TEM (JEOL, JEX-100CX) operated at 100 kV. The pigeonite grains show no fine structure such as exsolution and inversion. In many parts of the olivine grain, dislocations forming tilt boundaries and subgrain boundaries were observed (Fig. 8), and a metal crystal accompanied by dislocations was observed at the reduced rim. The chemical composition of a metal (Fe 99.7 wt%, Ni 0.3 wt%) which exists at the rim of the olivine grain was measured by analytical TEM (ATEM).

3.6. Mineralogy and chemistry of ALH-81101 and Y-790981

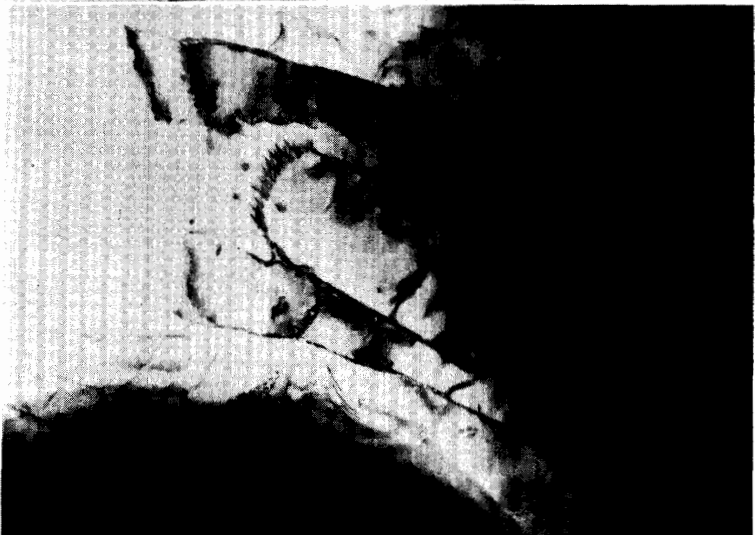
ALH-81101 (Fig. 9) and Y-790981 (Fig. 10) pigeonite crystals have a cloudy appearance due to fine glassy inclusions (Figs. 9b, 10a). The inclusions are micrometer-size glass and subcalcic diopside phases. The chemical compositions of Y-790981 pigeonites vary widely in the pyroxene quadrilateral because of the presence of inclusions, and the chemical compositions of the area which have no inclusions are centered at $\text{Ca}_9\text{Mg}_{72}\text{Fe}_{19}$ (Fig. 2). The chemical compositions of ALH-81101 pigeonites are similar to those of Y-790981 (Fig. 2). The variation of their chemical compositions is also due to inclusions and covers the entire range of known ureilites and extends towards the Mg end member (Fig. 2, Table 2). Their MnO/FeO ratios distribute almost on a horizontal line (Fig. 3).

ALH-81101 olivine crystals were originally 1–3 mm in diameter, but now show a granoblastic texture of smaller crystals (Fig. 9c). The olivine crystals in Y-790981

a. Subgrain boundaries. Bright field image. Width 5.8 μm .



b. Subgrain boundaries and tilt boundaries. Bright field image. Width 7.5 μm .



c. Screw dislocations around a metal grain. Bright field image. Width 3.0 μm .

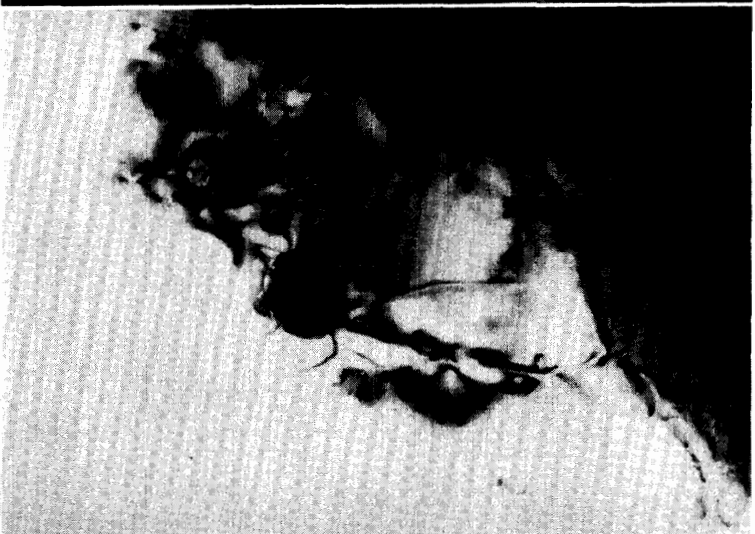
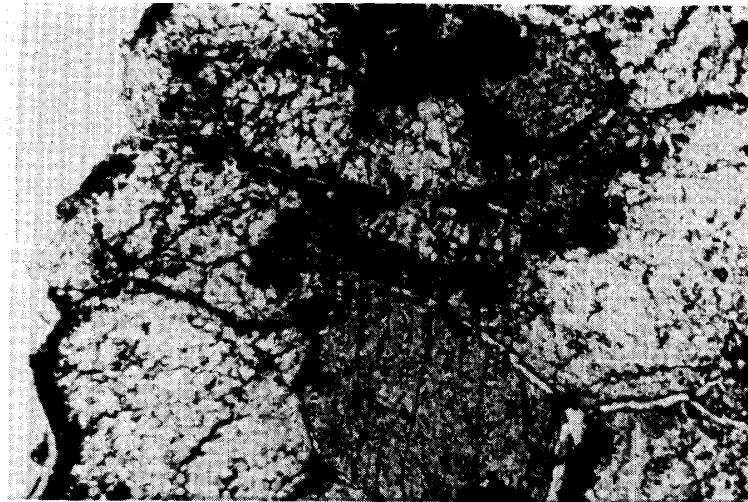
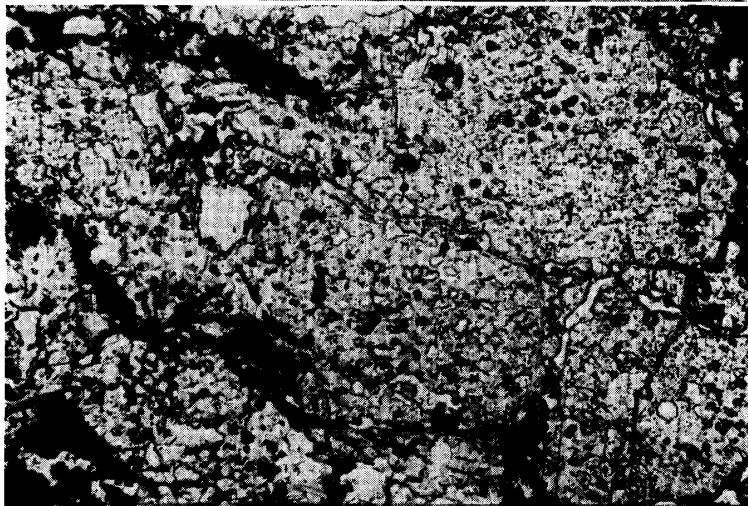


Fig. 8. Electron micrographs of dislocations in an olivine crystal in PCA82506.



a. Shocked textures of pigeonites and olivines. Plain light.



b. A cloudy pigeonite which has fine glassy inclusions. Plain light.



c. Granoblastic texture of an olivine crystal. Cross polarized light.

Fig. 9. Photomicrographs of ALH-81101. Width 0.95 mm.

a. *Cloudy pigeonites and carbonaceous matrix. Open.*



b. *Tilt boundaries in an olivine crystal. Cross polarized light.*

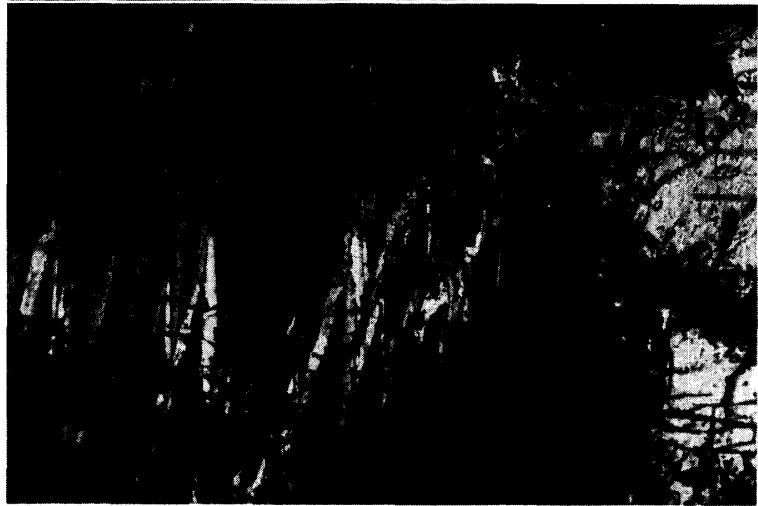


Fig. 10. Photomicrographs of Y-790981. Width 0.95 mm.

show undulatory extinction suggesting the presence of tilt boundaries (Fig. 10b). The variation of their chemical compositions is shown in Fig. 4.

4. Discussion

Mineralogical studies of PCA82506 revealed that this ureilite is relatively unshocked in comparison with others and that the modal abundance of pigeonite is nearly equal to that of olivine in spite of its low Fa content (DODD, 1981). This kind of ureilite is very rare especially among the larger ureilites and gives us an opportunity to study pigeonite and olivine by various mineralogical techniques.

The sharp spots and weak diffuse streaks on the diffraction photographs are in agreement with the petrographic texture, and suggest that PCA82506 has experienced only weak shock events. This finding has been confirmed by the TEM observation that no prominent shock features have been observed. On the contrary, many dislocation and subgrain boundary structures were observed in the olivine. In some areas of the ion-thinned specimen, well-developed tilt boundaries similar to those reported for ALH-78262 by MORI and TAKEDA (1983a) were recognized (Fig. 8). This

fact may suggest that dislocation recovery at high temperature to produce subgrain boundaries might have taken place for this ureilite as suggested for ALH-78262 by MORI and TAKEDA (1983a). In this study, a definite conclusion has not been reached, but future study may reveal useful information on the deformation and thermal history of the ureilite. There is the possibility that PCA82506 has experienced a heavy shock event but reheating to a high temperature has resulted in anneal shock textures.

The granoblastic texture of the ALH-81101 olivine crystal (Fig. 9c) suggests that the stress induced in the crystal is higher than that in PCA82506 and the duration of the high temperature episode of ALH-81101 was as long as or longer than that of PCA82506. The presence of glassy inclusions in the ALH-81101 and Y-790981 pigeonites (Figs. 9b, 10a) is also consistent with stronger shock heating of these meteorites. Their chemical variations (Figs. 2, 3) indicate that chemical fractionation of both major and minor elements took place during the high temperature episodes. This process may be significant in understanding the chemical variation on a more macroscopic scale observed in the known ureilites, because the macroscopic chemical trends are similar to those observed within a pigeonite crystal. (Figs. 2, 3).

The ATEM analysis of a metal grain in the PCA82506 olivine crystal shows that the metal (Fig. 8c) at the rim of the olivine contains minor Ni (Fe 99.7 wt%, Ni 0.3 wt%), and enstatite and forsterite are produced at the rim adjacent to the C-bearing matrix. Because primary metals at grain boundaries in other ureilites contain a few percent of Ni, we interpret that the low-Ni metal at the rim was produced from the olivine by reduction with carbon, and enstatite were produced by the same process. These facts support the boundary condition used to solve the diffusion equation.

The cooling rate, 10–15°C/h, obtained by the diffusion profile (MIYAMOTO *et al.*, 1985) is in agreement with that estimated for Y-74130 and Y-790981 pyroxenes (3 to 20°C/h) from the wavelength of the spinodal decomposition of Ca-rich pyroxenes by MORI and TAKEDA (1983b). These data indicate that the thermal history at the higher temperature than 800°C is very rapid cooling and that the Fe cations in only a limited area of olivine rim can be removed.

The cation distribution is influenced by chemical composition, minor element content, crystal structure, and multiple cooling histories (YAJIMA and HAFNER, 1974). It is generally understood that the variation in the concentration of Ca²⁺ in the M2 site significantly influences the distribution of Fe²⁺ and Mg²⁺ between the M1 and M2 sites. The equilibrium temperatures estimated by two distribution isotherms are shown in Table 5. The distribution isotherm shown in HAFNER *et al.* (1971) is based on the heating experiment data of chemically inhomogeneous pigeonites, which have exsolved augite lamellae. The distribution isotherm shown in SAXENA *et al.* (1974) is based on the heating experiment data of chemically homogeneous synthetic pigeonites without minor elements.

The equilibrium temperature based on SAXENA *et al.* (1974) indicates a higher value than that based on HAFNER *et al.* (1971). As shown in Table 5, the equilibrium temperatures of lunar samples, 12018 and 12053 from the same rock chip which should be equal, show different values. The data for 12053 are only 50°C different which is good while the data for 12018 are very different. There are two possible causes: (1) Pigeonites separated from lunar basalts include varied amounts of intergrown augite

or exsolved augite lamellae; (2) Most of the data shown in Table 5 are obtained by Mössbauer spectroscopy, and because about 50 mg powder samples are taken from polycrystalline mineral concentrates, the samples may be chemically inhomogeneous.

Our PCA82506 pigeonite is very homogeneous and the distribution isotherm (Fig. 7) by SAXENA *et al.* (1974), which is strictly applicable to chemically homogeneous pigeonites, is a preferred estimation of the equilibrium temperature. Although the PCA82506 pigeonite contains considerable amounts of Cr (Table 2), its influence on the estimated temperature is unknown at present. This temperature of 800°C suggests that PCA82506 pigeonite is cooled more rapidly than terrestrial ones from the Isle of Mull (MORIMOTO and GÜVEN, 1970). The PCA82506 value in Fig. 5 is located on the high temperature side of the distribution isotherm of known pigeonites (Fig. 5). The temperatures listed in Table 5, which may give a better temperature estimate than Fig. 5, also show that the last equilibrium temperature of the PCA82506 pigeonite is nearly equal to or a little lower than that of the most quickly cooled mare basalts. To obtain more precise values, heating experiments must be done in the future.

The quench temperature obtained from the Fe-Mg cation distribution of pigeonite suggests two cooling history models. One is the equilibrium temperature before rapid cooling, and the other is an apparent temperature when the cation distribution was fixed during the course of continuous cooling.

By combining cation distributions and diffusion data, we propose three models of the thermal history for PCA82506.

(1) Rapid cooling from 1250°C at a rate of 10–15°C/h to 800°C; after pyroxene equilibrium rapid cooling again.

(2) Rapid cooling from 1250°C to low temperature and then annealing at 800°C by a reheating event which allowed cation redistribution, then final rapid cooling.

(3) Rapid cooling from 1250°C at the rate of 10–15°C/h, and below 800°C continuous cooling with the cooling rate almost as rapid as the most quickly cooled mare basalts.

Process (3) is in good agreement with a hypothesis that the ureilite parent body experienced a breakup of the body at the end of its history.

Although existing data suggest that ureilites have undergone similar thermal history, the results obtained by studying PCA82506 will not apply to all. The above data are all that exist for ureilites and to estimate more precise cooling history, heating and cooling experiments with the PCA82506 pigeonite must be done. In addition, a time-temperature variation curve should be computed to estimate a position where the pigeonite crystal resided in the host rock. Taking all these data into consideration, we will gain a better understanding of the controversial cooling history of ureilite.

As previously indicated, several hypotheses for the origin of ureilites have been proposed. The previous discussion was based on qualitative estimates of cooling rate, but to make their origin clearer quantitative data values for temperature, time, pressure, cooling rate, etc. must be obtained.

Acknowledgments

We thank the Meteorite Working Group and NIPR for the samples, Dr. M.

MIYAMOTO for providing the diffusion profiles of computer simulation and Drs. Y. KUDO and H. MORI for helpful advice. This work was supported in part by the funds from Cooperative Program (No. 84134) provided by Ocean Research Institute, University of Tokyo. The electron microprobe work was carried out at Ocean Research Institute as part of this project.

References

- BEGEMANN, F. and OTT, U. (1983): Comment on "The nature and origin of ureilites" by J. L. Berkley *et al.* *Geochim. Cosmochim. Acta*, **47**, 975–977.
- BERKLEY, J. L., TAYLOR, G. J. and KEIL, K. (1978): Ureilites; Origin as related magmatic cumulates. *Lunar and Planetary Science IX*. Houston, Lunar Planet. Inst., 73–75.
- BERKLEY, J. L., TAYLOR, G. J., KEIL, K., HARLOW, G. E. and PRINZ, M. (1980): The nature and origin of ureilites. *Geochim. Cosmochim. Acta*, **44**, 1579–1597.
- BOYNTON, W. V., STARZYK, P. M. and SCHMITT, R. A. (1976): Chemical evidence for the genesis of the ureilites, the achondrite Chassigny and the nakhlites. *Geochim. Cosmochim. Acta*, **40**, 1439–1447.
- BROWN, G. E., PREWITT, C. T., PAPIKE, J. J. and SUENO, S. (1972): A comparison of the structures of low and high pigeonite. *J. Geophys. Res.*, **77**, 5778–5789.
- BROWN, G. E., WECHSLER, B. A. and WEIGAND, P. W. (1973): The crystal lography of pigeonites from basaltic vitrophyre 15597 (abstract). *Lunar Science IV*. Houston, Lunar Sci. Inst., 91–93.
- BUENING, D. K. and BUSECK, P. R. (1973): Fe-Mg lattice diffusion in olivine. *J. Geophys. Res.*, **78**, 6852–6862.
- CLARK, J. R., ROSS, M. and APPLEMAN, D. E. (1971): Crystal chemistry of a lunar pigeonite. *Am. Mineral.*, **56**, 888–908.
- CLIFF, G. and LORIMER, G. W. (1975): The quantitative analysis of thin specimens. *J. Microsc.*, **103**, 203–207.
- DODD, R. T. (1981): *Meteorites; A Petrologic-Chemical Synthesis*. Cambridge, Cambridge Univ. Press, 368 p.
- GHOSE, S., NG, G. and WALTER, L. S. (1972): Clinopyroxenes from Apollo 12 and 14; Exsolution, domain structure and cation order. *Proc. Lunar Sci. Conf.*, 3rd, 507–531.
- HAFNER, S. S., VIRGO, D. and WARBURTON, D. (1971): Cation distribution and cooling history of clinopyroxenes from Oceanus Procellarum. *Proc. Lunar Sci. Conf.*, 2nd, 91–108.
- LINDSLEY, D. H. and ANDERSON, D. J. (1983): A two-pyroxene thermometer. *Proc. Lunar Planet. Sci. Conf.*, 13th, Pt. 2, A887–A906 (*J. Geophys. Res.*, **88** Suppl.).
- MASON, B. (1983): *Antarct. Meteorite Newsl.*, **6**.
- MIYAMOTO, M., TAKEDA, H. and TOYODA, H. (1985): Cooling history of some Antarctic ureilites. *Proc. Lunar Planet. Sci. Conf.*, 16th, Pt. 1, D116–D122 (*J. Geophys. Res.*, **90** Suppl.).
- MORI, H. and TAKEDA, H. (1983a): Deformation of olivine in the Antarctic ureilites, Allan Hills 77257 and 78262 (abstract). *Lunar and Planetary Science XIV*. Houston, Lunar Planet. Inst., 519–520.
- MORI, H. and TAKEDA, H. (1983b): An electron petrographic study of ureilite pyroxenes (abstract). *Meteoritics*, **18**, 358–359.
- MORIMOTO, M. and GÜVEN, N. (1970): Refinement of the crystal structure of pigeonite. *Am. Mineral.*, **55**, 1195–1209.
- SASAKI, S. (1982): Full-matrix least squares program, RADY, modification of the program "ORFLS" by BUSING, W. R. and LEVY, H. A. (1959) CF Memo 59–4–37, Oak Ridge National Laboratory, Oak Ridge, Tennessee, April, 1959 and "RADIEL" by P. Coppens *et al.* (1979) *Acta Crystallogr.*, Ser. A, **35**, 63–72. Program Library, Mineral. Inst., Univ. of Tokyo.
- SAXENA, S. K., GHOSE, S. and TURNOCK, A. C. (1974): Cation distribution in low-calcium pyroxenes; Dependence on temperature and calcium content and the thermal history of lunar and terrestrial pigeonites. *Earth Planet. Sci. Lett.*, **21**, 194–200.

- TAKEDA, H. (1972): Substructural studies of rim augite and core pigeonite from lunar rocks 12502. *Earth Planet. Sci. Lett.*, **15**, 65–71.
- TAKEDA, H. and TACHIKAWA, O. (1984): Some new ureilites and a working hypothesis on the origin of ureilites. *Proc. 17th ISAS Lunar Planet. Symp.* Tokyo, Inst. Space Astron. Sci., 41–42.
- TAKEDA, H. and YANAI, K. (1982): Mineralogical examination of the Yamato-79 achondrites; Polymict eucrites and ureilites. *Mem. Natl Inst. Polar Res., Spec. Issue*, **25**, 97–123.
- TAKEDA, H., MORI, H., YANAI, K. and SHIRAISHI, K. (1980): Mineralogical examination of the Allan Hills achondrites and their bearing on the parent bodies. *Mem. Natl Inst. Polar Res., Spec. Issue*, **17**, 119–144.
- VDOVYKEN, G. P. (1970): Ureilites. *Space Sci. Rev.*, **10**, 483–510.
- VIRGO, D. (1973): Clinopyroxenes from Apollo 15; Fe²⁺, Mg intracrystalline distributions (abstract). *Lunar Science IV.* Houston, Lunar Sci. Inst., 749–751.
- YAJIMA, T. and HAFNER, S. S. (1974): Cation distribution and equilibrium temperature of pigeonite from basalt 15065. *Proc. Lunar Sci. Conf.*, 5th, 769–784.

(Received July 3, 1985; Revised manuscript received October 17, 1985)